

Be Your Own Neighborhood: Detecting Adversarial Example by the Neighborhood Relations Built on Self-Supervised Learning

Zhiyuan He ^{1*}, Yijun Yang ^{1*}, Pin-Yu Chen ², Qiang Xu ¹, Tsung-Yi Ho ¹

¹Department of Computer Science and Engineering, The Chinese University of Hong Kong

²IBM Research

{zyhe, yjyang, qxu, tyho}@cse.cuhk.edu.hk, pin-yu.chen@ibm.com

Abstract

Deep Neural Networks (DNNs) have achieved excellent performance in various fields. However, DNNs' vulnerability to Adversarial Examples (AE) hinders their deployments to safety-critical applications. This paper presents a novel AE detection framework, named **BEYOND**, for trustworthy predictions. **BEYOND** performs the detection by distinguishing the AE's abnormal relation with its augmented versions, i.e. neighbors, from two prospects: representation similarity and label consistency. An off-the-shelf Self-Supervised Learning (SSL) model is used to extract the representation and predict the label for its highly informative representation capacity compared to supervised learning models. For clean samples, their representations and predictions are closely consistent with their neighbors, whereas those of AEs differ greatly. Furthermore, we explain this observation and show that by leveraging this discrepancy **BEYOND** can effectively detect AEs. We develop a rigorous justification for the effectiveness of **BEYOND**. Furthermore, as a plug-and-play model, **BEYOND** can easily cooperate with the Adversarial Trained Classifier (ATC), achieving the state-of-the-art (SOTA) robustness accuracy. Experimental results show that **BEYOND** outperforms baselines by a large margin, especially under adaptive attacks. Empowered by the robust relation net built on SSL, we found that **BEYOND** outperforms baselines in terms of both detection ability and speed. *Our code will be publicly available.*

1 Introduction

Deep Neural Networks (DNNs) have been widely adopted in many fields due to their superior performance. However, DNNs are vulnerable to Adversarial Examples (AEs), which can easily fool DNNs by adding some imperceptible adversarial perturbations. This vulnerability prevents DNN from being deployed in safety-critical applications such as autonomous driving (Cococcioni et al. 2020) and disease diagnosis (Kaissis et al. 2022), where incorrect predictions can lead to catastrophic economic and even loss of life.

Existing defensive countermeasures can be roughly categorized as: adversarial training, input purification (Mao et al. 2021), and AE detection (Xu, Evans, and Qi 2017). Adversarial training is known as the most effective defense technique (Croce and Hein 2020), but it brings about degradation of accuracy and additional training cost, which are

unacceptable in some application scenarios. In contrast, input transformation techniques without high training / deployment costs, but their defensive ability is limited, i.e. easily defeated by adaptive attacks (Croce and Hein 2020).

Recently, a large number of AE detection methods have been proposed. Some methods detect AE by interrogating the abnormal relationship between AE and other samples. For example, Deep k-Nearest Neighbors (DkNN) (Papernot and McDaniel 2018) compares the DNN-extracted features of the input image with those of its k nearest neighbors layer by layer to identify AE, leading to a high inference cost. Instead of comparing all features, Latent Neighborhood Graph (LNG) (Abusnaina et al. 2021) employs a Graph Neural Network to make the comparison on a neighborhood graph, whose nodes are pre-stored embeddings of AEs together with those of the clean ones extracted by DNN, and the edges are built according to distances between the input node and every reference node. Though more efficient than DkNN, LNG suffers from some weaknesses: some AE samples are required to build the graph the detection performance relays on the reference AEs and cannot effectively generalize to unseen attacks. More importantly, both DkNN and LNG can be bypassed by adaptive attacks, in which the adversary has full knowledge of the detection strategy.

We observe that one cause for adversarial vulnerability is the lack of feature invariance (Jiang et al. 2020), i.e., small perturbations may lead to undesired large changes in features or even predicted labels. Self-Supervised Learning (SSL) (Chen and He 2021) models learn data representation consistency under different data augmentations, which intuitively can mitigate the issue of lacking feature invariance and thus improve adversarial robustness. As an illustration, we visualize the SSL-extracted representation of the clean sample, AE and that of their corresponding augmentations in Fig. 1 (right). We can observe that the clean sample has closer ties with its neighbors, reflected by the higher label consistency and representation similarity. However, the AE representation stays quite far away from its neighbors, and there is a wide divergence in the predicted labels.

Inspired by the above observations, we propose a novel AE detection framework, named **BE Your Own Neighborhood** (**BEYOND**). The contributions of this work are summarized as follows:

- We propose **BEYOND**, a novel AE detection framework,

*These authors contributed equally.

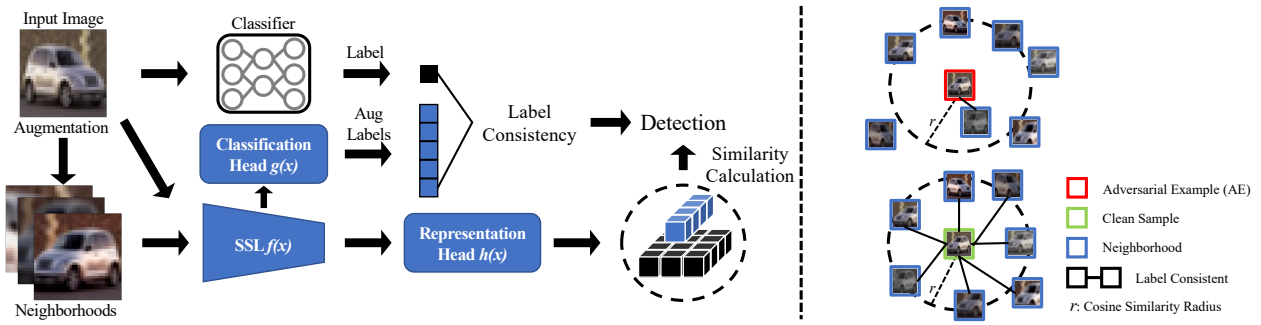


Figure 1: Pipeline of the proposed **BEYOND** framework. First we augment the input image to obtain a bunch of its neighbors. Then, we perform the label consistency detection mechanism on the classifier’s prediction of the input image and that of neighbors predicted by SSL’s classification head. Meanwhile, the representation similarity mechanism employs *cosine distance* to measure the similarity among the input image and its neighbors (left). The input image with poor label consistency or representation similarity is flagged as AE (right).

which takes advantage of SSL model’s robust representation capacity to identify AE by referring to its neighbors. To our best knowledge, BEYOND is the first work that leverages SSL model for AE detection without prior knowledge of adversarial attacks or AEs.

- We develop a rigorous justification for the effectiveness of BEYOND, and we derive an indicator to evaluate the validity of the candidate augmentation.
- BEYOND can defend effectively against adaptive attacks. To defeat the two detection mechanisms: label consistency and representation similarity simultaneously, attackers have to optimize two objectives with contradictory directions, resulting in gradients canceling each other out.
- As a plug-and-play method, BEYOND can be applied directly to any image classifier without compromising accuracy or additional retraining costs.

Experimental results show that BEYOND outperforms baselines by a large margin, especially under adaptive attacks. Empowered by the robust relation net built on SSL, we found BEYOND outperforms baselines in terms of both detection ability and implementation costs.

2 Related Works

(Szegedy et al. 2013) first discover that an adversary could maximize the prediction error of the network by adding some imperceptible perturbation, δ , which is typically bounded by a perturbation budget, ϵ , under a L_p -norm, e.g., L_∞ , L_2 . Project Gradient Descent (PGD) proposed by (Madry et al. 2017) is one of the most powerful iterative attacks. PGD motivates various gradient-based attacks such as AutoAttack (Croce and Hein 2020) and Orthogonal-PGD (Bryniarski et al. 2021), which can break many SOTA AE defenses (Croce et al. 2022). Another widely adopted adversarial attack is C&W (Carlini and Wagner 2017). Compared to the norm-bounded PGD attack, C&W conducts AEs with a high attack success rate by formulating the adversarial attack problem as an optimization problem.

Existing defense techniques focus either on robust prediction or detection. The most effective way to achieve robust prediction is adversarial training (Zhang et al. 2019; Elfwing,

Uchibe, and Doya 2018), and the use of nearest neighbors is a common approach to detecting AEs. kNN (Dubey et al. 2019) and DkNN (Papernot and McDaniel 2018) discriminate AEs by checking the label consistency of each layer’s neighborhoods. (Ma et al. 2018) define Local Intrinsic Dimensionality (LID) to characterize the properties of AEs and use a simple k-NN classifier to detect AEs. LNG (Abusnaina et al. 2021) searches for the nearest samples in the reference data and constructs a graph, further training a specialized GNN to detect AEs. Although these nearest-neighbor-based methods achieve competitive detection performance, all rely on external AEs for training detectors or searching thresholds, resulting in defeat against unseen attacks.

Recent studies have shown that SSL can improve adversarial robustness as SSL models are label-independent and insensitive to transformations (Hendrycks et al. 2019b). An intuitive idea is to combine adversarial training and SSL (Kim, Tack, and Hwang 2020) (Ho and Nvasconcelos 2020), which remain computationally expensive and not robust to adaptive attacks. (Shi, Holtz, and Mishne 2021) and (Mao et al. 2021) find that the auxiliary SSL task can be used to purify AEs, which are shown to be robust to adaptive attacks. However, (Croce et al. 2022) show that these purification methods can be broken by stronger adaptive attacks.

3 Proposed Method

3.1 Method Overview

Components. BEYOND consists of three components: a SSL feature extractor $f(\cdot)$, a classification head $g(\cdot)$, and a representation head $h(\cdot)$, as shown in Fig. 1 (left). Specifically, the SSL feature extractor is a Convolutional Neural Network (CNN), pre-trained by specially designed loss, e.g. contrastive loss, without supervision¹. A Fully-Connected layer (FC) acts as the classification head $g(\cdot)$, trained by freezing the $f(\cdot)$. The $g(\cdot)$ performs on the input image’s neighbors for label consistency detection. The representation head $h(\cdot)$ consisting of three FCs, encodes the output of $f(\cdot)$

¹Here, we employ the SimSiam (Chen and He 2021) as the SSL feature-extractor for its decent performance.

Algorithm 1: BEYOND detection algorithm

- 1 **Input:** Input image x , target classifier $c(\cdot)$, SSL feature extractor $f(x)$, classification head $g(x)$, projector head $h(x)$, label consistency threshold \mathcal{T}_{label} , representation similarity threshold \mathcal{T}_{rep} , Augmentation Aug , neighbor indicator i , total neighbor k
 - 2 **Output:** reject / accept
 - 1: **Stage1: Collect labels and representations.**
 - 2: $\ell_{cls}(x) = c(x)$
 - 3: **for** i in k **do**
 - 4: $\hat{x}_i = Aug(x)$
 - 5: $\ell_{ssl}(\hat{x}_i) = f(g(\hat{x}_i)); r(x) = f(h(x)); r(\hat{x}_i) = f(h(\hat{x}_i))$
 - 6: **Stage2: Label consistency detection mechanism.**
 - 7: **for** i in k **do**
 - 8: **if** $\ell(\hat{x}_i) == \ell(x)$ **then** $Ind_{label} += 1$
 - 9: **Stage3: Representation similarity detection mechanism.**
 - 10: **for** i in k **do**
 - 11: **if** $\cos(r(x), r(\hat{x}_i)) < \mathcal{T}_{cos}$ **then** $Ind_{rep} += 1$
 - 12: **Stage4: AE detection.**
 - 13: **if** $Ind_{label} < \mathcal{T}_{label}$ or $Ind_{rep} < \mathcal{T}_{rep}$ **then** reject
 - 14: **else** accept
-

to an embedding, i.e. representation. We operate the representation similarity detection between the input image and its neighbors.

Core idea. Our approach relies on robust relationships between the input and its neighbors for the detection of AE. The key idea is that adversaries may easily attack one sample’s representation to another submanifold, but it is difficult to totally shift that of all its neighbors. We employ the SSL model to capture such relationships, since it is trained to project input and its augmentations (neighbors) to the same submanifold (Chen and He 2021).

Selection of neighbor number. Obviously, the larger the number of neighbors, the more stable the relationship between them, but this may increase the overhead. We choose 50 neighbors for BEYOND, since larger neighbors no longer significantly enhance performance, as shown in Fig. 2.

Workflow. Fig. 1 shows the workflow of the proposed BEYOND. When input comes, we first transform it into 50 augmentations, i.e. 50 neighbors. Note that BEYOND is not based on random data augmentation. Next, the input along with its 50 neighbors are fed to SSL feature extractor $f(\cdot)$ and then the classification head $g(\cdot)$ and the representation head $h(\cdot)$, respectively. For the classification branch, $g(\cdot)$ outputs the predicted label for 50 neighbors. Later, the label consistency detection algorithm calculates the consistency level between the input label (predicted by the classifier) and 50 neighbor labels. When it comes to the representation branch, the 51 generated representations are sent to the representation similarity detection algorithm for AE detection. If the consistency of the label of a sample or its representation similarity is lower than a threshold, BEYOND shall flag it AE.

3.2 Detection Algorithms

For enhanced AE detection capability, BEYOND adopted two detection mechanisms: *Label Consistency*, and *Representa-*

tion Similarity. The detection performance of the two combined can exceed any of the individuals. More importantly, their contradictory optimization directions hinder adaptive attacks to bypass both of them simultaneously.

Label Consistency. We compare the classifier prediction, $\ell_{cls}(x)$, on the input image, x , with the predictions of the SSL classification head, $\ell_{ssl}(\hat{x}_i), i = 1 \dots k$, where \hat{x}_i denotes the i th neighbor, k is the total number of neighbors. If $\ell_{cls}(x)$ equals $\ell_{ssl}(\hat{x}_i)$, the label consistency increases by one, $Ind_{Label} += 1$. Once the final label consistency is less than the threshold, $Ind_{Label} < \mathcal{T}_{label}$, the *Label Consistency* flags it as AE. We summarize the label consistency detection mechanism in Algorithm. 1.

Representation Similarity. We employ the *cosine distance* as a metric to calculate the similarity between the representation of input sample $r(x)$ and that of its neighbors, $r(\hat{x}_i), i = 1, \dots, k$. Once the similarity, $-\cos(r(x), r(\hat{x}_i))$, is higher than a certain value, representation similarity increases by 1, $Ind_{Rep} += 1$. If the final representation similarity is less than a threshold, $Ind_{Rep} < \mathcal{T}_{rep}$, the *representation similarity* flag the sample as an AE. Algorithm. 1 concludes the representation similarity detection mechanism.

Note that, we select the thresholds, i.e. $\mathcal{T}_{label}, \mathcal{T}_{rep}$, by fixing the False Positive Rate (FPR)@5%, which can be determined only by clean samples, and the implementation of our method needs no prior knowledge about AE.

3.3 Resistance to Adaptive Attacks

Attackers may design adaptive attacks to bypass BEYOND, if attackers know both the classifier and the detection strategy. BEYOND apply augmentations on the input, weakening adversarial perturbations. As a result, to fool SSL’s classification results on neighbors, i.e. bypass label consistency detection, large perturbations are needed. However, the added perturbation should be small to bypass the representation similarity detection, since a large perturbation can alter the representation significantly. Therefore, to attack BEYOND, attackers have to optimize two objectives that have contradictory directions, resulting in gradients canceling each other out.

4 Theoretical Justification

Our proposed method is based on the observation that the similarity between AE and its neighbors (augmentations) is significantly smaller than that of the clean sample in the feature space of the SSL model. This section provides theoretical support for the above observation. For ease of exposition, our analysis is built on a first-order approximation of nonlinear neural networks, employs $\|\cdot\|_2$ to represent similarity, and considers the linear data augmentation.

Theoretical analysis. Given a clean sample x , we receive its feature $f(x)$ lying in the feature space spanned by the SSL model. We assume that benign perturbation, i.e. random noise, $\hat{\delta}$, with bounded budgets causes minor variation, $\hat{\epsilon}$, on the feature space, as described in Eq. 1:

$$f(x + \hat{\delta}) = f(x) + \nabla f(x)\hat{\delta} = f(x) + \hat{\epsilon}, \quad (1)$$

where $\|\hat{\epsilon}\|_2$ is constrained to be within a radius r . In contrast, when it comes to AE, x_{adv} , the adversarial perturbation, δ ,

can cause considerable change, due to its maliciousness, that is, it causes misclassification and transferability (Papernot, McDaniel, and Goodfellow 2016; Demontis et al. 2019; Liu et al. 2021), as formulated in Eq. 2.

$$f(x_{adv}) = f(x + \delta) = f(x) + \nabla f(x)\delta = f(x) + \varepsilon, \quad (2)$$

where $\|\varepsilon\|_2$ is significantly larger than $\|\hat{\varepsilon}\|_2$ formally, $\lim_{\hat{\varepsilon} \rightarrow 0} \frac{\|\varepsilon\|_2}{\|\hat{\varepsilon}\|_2} = \infty$. SSL model is trained to generate close representations for an input x and its augmentation $x_{aug} = Wx$ (Jaiswal et al. 2020; Hendrycks et al. 2019a), where $W \in \mathbb{R}^{w \times h}$, w, h denote the width and height of x , respectively. Based on this natural property of SSL, we have:

$$f(Wx) = f(x) + o(\hat{\varepsilon}), \nabla f(Wx) = \nabla f(x) + o(\hat{\varepsilon}), \quad (3)$$

where $o(\hat{\varepsilon})$ is a high-order infinitesimal item of $\hat{\varepsilon}$. Moreover, according to Eq. 1 and Eq. 3, we can derive that:

$$\begin{aligned} f(W(x + \hat{\delta})) &= f(Wx) + \nabla f(Wx)W\hat{\delta} \\ &= f(x) + \nabla f(x)W\hat{\delta} + o(\hat{\varepsilon}). \end{aligned} \quad (4)$$

We let $\hat{\varepsilon}_{aug} = \nabla f(x)W\hat{\delta}$ and assume $\hat{\varepsilon}_{aug}$ and $\hat{\varepsilon}$ are infinitesimal isotropic, i.e. $\lim_{\hat{\varepsilon} \rightarrow 0} \frac{\hat{\varepsilon}_{aug}}{\hat{\varepsilon}} = c$, where c is a constant. Therefore, we can rewrite Eq. 4 as follows:

$$f(W(x + \hat{\delta})) = f(x) + c \cdot \hat{\varepsilon} + o(\hat{\varepsilon}). \quad (5)$$

Our goal is to prove that *distance (similarity) between AE and its neighbors can be significantly smaller (larger) than that of the clean sample in the space spanned by a SSL model*, which is equivalent to justify Eq. 6

$$\|f(x_{adv}) - f(W(x_{adv}))\|_2^2 \geq \underbrace{\|f(x) - f(Wx)\|_2^2}_{\hat{\varepsilon}_{aug}=c \cdot \hat{\varepsilon}}. \quad (6)$$

Expanding the left-hand item in Eq. 6, and defining $m = \nabla f(x)W\delta$, we can obtain the following.

$$\begin{aligned} \|f(x_{adv}) - f(Wx_{adv})\|_2^2 &= \|f(x + \delta) - f(W(x + \delta))\|_2^2 \\ &= \|f(x) + \nabla f(x)\delta - f(Wx) - \nabla f(Wx)W\delta\|_2^2 \\ &= \|\varepsilon - \nabla f(x)W\delta - o(\varepsilon)\|_2^2 = \|\varepsilon\|_2^2 + \|m\|_2^2 - 2\langle \varepsilon, m \rangle + o(\varepsilon) \end{aligned} \quad (7)$$

As mentioned in the prior literature (Mikołajczyk and Grochowski 2018; Zeng et al. 2020; Raff et al. 2019), augmentations can effectively weaken adversarial perturbation δ . Therefore, we assume that the influence caused by $W\delta$ is weaker than δ but stronger than the benign perturbation, $\hat{\delta}$. Formally, we have:

$$\|\underbrace{\nabla f(x)\delta}_{\varepsilon}\|_2 > \|\underbrace{\nabla f(x)W\delta}_m\|_2 > \|\underbrace{\nabla f(x)W\hat{\delta}}_{\hat{\varepsilon}_{aug}=c \cdot \hat{\varepsilon}}\|_2. \quad (8)$$

According to *Cauchy-Schwarz inequality* (Bhatia and Davis 1995), we have the following chain of inequalities obtained by taking Eq. 8 into Eq. 7:

$$\begin{aligned} \|\varepsilon\|_2^2 + \|m\|_2^2 - 2\langle \varepsilon, m \rangle + o(\varepsilon) &> \\ \|\varepsilon\|_2^2 + \|m\|_2^2 - 2\|\varepsilon\| \cdot \|m\| &= (\|\varepsilon\|_2 - \|m\|_2)^2, \end{aligned} \quad (9)$$

where $\|m\| \in (\|\hat{\varepsilon}_{aug}\|, \|\varepsilon\|)$ according to Eq. 8.

Finally, from Eq. 9 we observe that by applying proper data augmentation, the distance between AE and its neighbors in SSL's feature space $\|f(x_{adv}) - f(Wx_{adv})\|_2 = \|\varepsilon\|_2 - \|m\|_2$ can be significantly larger than that of clean samples $\|f(x) - f(Wx)\|_2 = o(\hat{\varepsilon})$. The enlarged distance is upper bounded by $\|\varepsilon\|_2 / \|\hat{\varepsilon}_{aug}\|_2$ times that of clean sample, which implies that the imperceptible perturbation δ in the image space can be significantly enlarged in SSL's feature space by referring to its neighbors. This exactly supports the design of BEYOND as described in Section 3.1. In practice, we adopt various augmentations instead of a single type to generate multiple neighbors for AE detection, which reduces the randomness, resulting in more robust estimations.

Select effective augmentations. To better improve the effectiveness of BEYOND, we analyze the conditions under which the augmentation can effectively weaken adversarial perturbation. Effective data augmentation makes the augmented label y_{aug} tend to the ground-truth label y_{true} and away from the adversarial label y_{adv} :

$$\|y_{aug} - y_{true}\|_2 \leq \|y_{aug} - y_{adv}\|_2 \leq \|y_{adv} - y_{true}\|_2. \quad (10)$$

Since y_{true} is the hard label (one-hot encoding), the range of $\|y_{adv} - y_{true}\|_2$ is $(\sqrt{2}/2, \sqrt{2})$. The distance is $\sqrt{2}$ when the item corresponding to y_{adv} is 1 in the logits of y_{adv} , and $\sqrt{2}/2$ when the item corresponding to y_{adv} and y_{true} both occupy 1/2. Given a SSL-based classifier, C , we have:

$$\begin{aligned} C(W(x + \delta)) &= C(Wx) + \nabla C(Wx)W\delta \\ &= y_{true} + \nabla C(Wx)W\delta = y_{aug}. \end{aligned} \quad (11)$$

Therefore, the distance between y_{aug} and y_{true} is:

$$\begin{aligned} \|y_{aug} - y_{true}\|_2 &= \|\nabla C(Wx)W\delta\|_2 \\ &\leq \|\nabla C(Wx)W\|_2 \|\delta\|_2 \leq \|\nabla C(Wx)W\|_2 \varepsilon, \end{aligned} \quad (12)$$

where $\|\delta\|_2$ is bounded by ε . Eq. 10 always holds, then:

$$\|\nabla C(Wx)W\|_2 \varepsilon \leq \frac{\sqrt{2}}{2} \Rightarrow \|\nabla C(Wx)W\|_2 \leq \frac{\sqrt{2}}{2\varepsilon}. \quad (13)$$

In summary, augmentation can mitigate adversarial perturbation when it satisfies Eq. 13. We find *color jitter* and *rotation* are most effective in terms of Eq. 13 among all the tested data augmentations. For space limitations, we leave the detailed comparison on data augmentations in Appendix.

5 Evaluation

5.1 Experimental Setting

Gray-box attack & White-box attack. In the gray-box attack setting, the adversary has complete knowledge of the classifier, while the detection strategy is confidential. Whereas in an adaptive attack (white-box) setting, the adversary is aware of the detection strategy.

Datasets & Target models. We conduct experiments on three commonly adopted datasets including CIFAR-10 (Krizhevsky, Hinton et al. 2009), CIFAR-100, and a more IMAGENET (Krizhevsky, Sutskever, and Hinton 2012). The details of the target models (classifiers), and the employed

SSL models together with their original classification accuracy on clean samples are summarized in Tab. 1².

Dataset	Classifier SSL	Acc. on clean samples [↑]	
		Classifier	SSL
CIFAR-10	ResNet18	91.53%	90.74%
CIFAR-100	ResNet18	75.34%	66.04%
IMAGENET	ResNet50	80.86%	68.30%

Table 1: Information of datasets and models.

Attacks. Gray-box evaluations are conducted on FGSM, PGD, C&W, and AutoAttack. AutoAttack includes APGD, APGD-T, FAB-T, and Square (Andriushchenko et al. 2020), where APGD-T and FAB-T are targeted attacks and Square is a black-box attack. As for adaptive attacks, we employed the most adopted PGD and Orthogonal-PGD, which is a recent adaptive attack designed for AE detectors.

Metrics. Following previous works (Yang et al. 2022; Abusnaina et al. 2021) we employ TPR@FPR, ROC curve & AUC, and robust accuracy (RA) as evaluation metrics.

- **TPR@FPR:** TPR@FPR indicates the true positive rate (TPR) at a false positive rate (FPR) $\leq n\%$, which is used as the primary metric to assess detector performance.
- **ROC curve & AUC:** Receiver Operating Characteristic (ROC) curves describe the impact of various thresholds on detection performance, and the Area Under the Curve (AUC) is an overall indicator of the ROC curve.
- **Robust Accuracy (RA):** We employ RA as an evaluation metric, which can reflect the overall system performance against adaptive attacks by considering both the classifier and the detector.

Baselines. We choose five detection-based defense methods as baselines: kNN, DkNN, LID, (Hu et al. 2019) and LNG, which also consider the relationship between the input and its neighbors to some extent.

5.2 Defending Gray-box Attacks

Tab. 2 reports TPR@FPR5% to show the AE detection performance of BEYOND. It can be observed that BEYOND maintains a high detection performance on various attacks and datasets, which is attributed to our detection mechanism. Combining label consistency and representation similarity, BEYOND identifies AEs without reference AE set. For more results of TPR@FPR3%, please refer to Appendix.

²The pre-trained SSL models for CIFAR-10 and CIFAR-100 are from Solo-learn (da Costa et al. 2022), and for IMAGENET are from SimSiam (Chen and He 2021).

Dataset	CIFAR-10	CIFAR-100	IMAGENET
Attack	TPR@FPR5%[↑]		
FGSM	86.16%	89.80%	61.05%
PGD	82.80%	85.90%	89.80%
C&W	91.48%	91.96%	76.69%
AutoAttack	93.42%	90.90%	84.25%

Table 2: TPR@FPR 5% of BEYOND against Gray-box Attacks. All attacks are performed under $L_\infty = 8/255$.

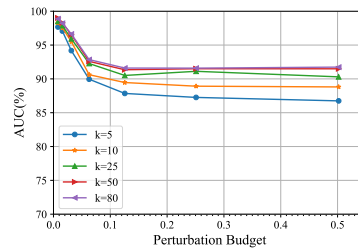


Figure 2: Detection performance with different number of neighbors on CIFAR-10.

Model	Acc. on clean samples		RA	
	ATC	ATC+BEYOND	ATC	ATC+BEYOND
R2021Fixing70	92.23%	92.83%	66.20%	84.40%
G2021Improving70	88.74%	90.81%	64.10%	81.50%
G2020Uncovering70	91.10%	91.79%	64.70%	83.80%
R2021Fixing106	88.50%	90.51%	62.20%	81.30%

Table 3: ATC+BEYOND against AutoAttack on CIFAR-10.

Fig. 2 shows the effect of the number of neighbors on the detection performance against PGD with different perturbation budgets. It can be observed that the detection performance with a large number of neighbors is better, but the performance is not significantly improved when the number of neighbors exceeds 50. In addition, previous methods argue that the detection of small perturbations is challenging (Abusnaina et al. 2021). However, it’s shown that BEYOND has better detection performance for small perturbations, and maintains a high level of detection performance for large perturbations. This is because previous distance-measure-based methods are not sensitive to small perturbations, which BEYOND avoids by combining differences in high-dimensional representations and semantics (label consistency).

Combined With ATC As a plug-and-play approach, BEYOND integrates well with existing Adversarial Trained Classifier (ATC)³. Tab. 3 shows the accuracy on clean samples and RA against AutoAttack of ATC combined with BEYOND on CIFAR-10. As can be seen the addition of BEYOND increases the robustness of ATC by a significant margin on both clean samples and AEs.

Comparison with Existing Methods Tab. 4 compares the AUC of BEYOND with five AE detection methods: DkNN, kNN, LID, Hu et al., and LNG on CIFAR-10. Since LID and LNG rely on reference AEs, we report detection performance on both seen and unseen attacks. In the seen attack setting, LID and LNG are trained with all types of attacks, while using only the C&W attack in the unseen attack setting. Note that the detection performance for seen and unseen attacks is consistent for detection methods without AEs training.

Experimental results show that BEYOND consistently outperforms SOTA AE detectors, and the performance advantage is particularly significant when detecting unseen attacks. This is because BEYOND uses the augmentations of the input as its neighbors without relying on prior adversarial knowledge.

³All ATCs are sourced from RobustBench (Croce et al. 2020).

Methods	<i>Unseen</i> : Attacks used in training are preclude from tests.				<i>Seen</i> : Attacks used in training are included in tests.				
	FGSM	PGD	AutoAttack	Square	FGSM	PGD	CW	AutoAttack	Square
DkNN	61.50%	51.18%	52.11%	59.51%	61.50%	51.18%	61.46%	52.11%	59.21%
kNN	61.80%	54.46%	52.64%	73.39%	61.80%	54.46%	62.25%	52.64%	73.39%
LID	71.15%	61.27%	55.57%	66.11%	73.56%	67.95%	55.60%	56.25%	85.93%
Hu	84.44%	58.55%	53.54%	<u>95.83%</u>	84.44%	58.55%	<u>90.99%</u>	53.54%	95.83%
LNG	<u>98.51%</u>	<u>63.14%</u>	<u>58.47%</u>	94.71%	99.88%	<u>91.39%</u>	89.74%	<u>84.03%</u>	<u>98.82%</u>
BEYOND	98.89%	99.29%	99.18%	99.29%	<u>98.89%</u>	99.29%	99.20%	99.18%	99.29%

Table 4: The AUC of Different Adversarial Detection Approaches on CIFAR-10. To align with baselines, classifier: ResNet110, FGSM: $\epsilon = 0.05$, PGD: $\epsilon = 0.02$. Note that **BEYOND needs no AE for training**, leading to the same value on both *seen* and *unseen* settings. The **bolded** values are the best performance, and the underlined italicized values are the second-best performance, the same below.

α	0	1	10	20	50	100
CIFAR-10	82.03%	63.91%	64.57%	76.15%	88.56%	92.53%
CIFAR-100	90.58%	88.49%	91.61%	93.10%	94.05%	94.37%

Table 5: AUC for Adaptive Attack under different α (Eq.15).

And according to the conclusion in Sec. 4, adversarial perturbations impair label consistency and representation similarity, which enables BEYOND to distinguish AEs from benign ones with high accuracy. For more comparative results on IMAGENET, please refer to the Appendix.

5.3 Defending Adaptive Attacks

Adaptive Objective Loss Function. Attackers can design adaptive attacks to bypass BEYOND when the attacker knows all the parameters of the model and the detection strategy. To attack effectively, the adversary must deceive the target model while guaranteeing the label consistency and representation similarity of the SSL model. Since BEYOND uses multiple augmentations, we consider the impact of all augmentations on label consistency and representation similarity during the attack, and conduct the following adaptive attack objective items as suggested by (Athalye et al. 2018):

$$\begin{aligned}
 Sim_l &= \frac{1}{k} \sum_{i=1}^k \mathcal{L} \left(C \left(W^i(x + \delta) \right), y_t \right) \\
 Sim_r &= \frac{1}{k} \sum_{i=1}^k (\mathcal{S}(r(W^i(x + \delta)), r(x + \delta))),
 \end{aligned} \tag{14}$$

where \mathcal{S} represents cosine similarity, and adaptive adversaries perform attacks on the following objective function:

$$\min_{\delta} \mathcal{L}_C(x + \delta, y_t) + Sim_l - \alpha \cdot Sim_r, \tag{15}$$

where \mathcal{L}_C indicates classifier’s loss function, y_t is the targeted class, δ denotes the adversarial perturbation, and α refers to a hyperparameter⁴. The design of the adaptive attack in Eq. 15 includes a hyperparameter α , which is a trade-off parameter between label consistency and representation similarity. Tab. 5 shows the AUC of BEYOND under different α . As shown, when $\alpha = 0$, i.e. the attacker only attacks the label consistency detection mechanism, the AUC score is still high, which proves that our approach is not based on the weak transferability of AEs. Moreover, adaptive attacks are strongest when $\alpha = 1$, which is used for rest tests.

⁴Note that we employ cosine metric is negatively correlated the similarity, so that the Sim_r item is preceded by a minus sign.

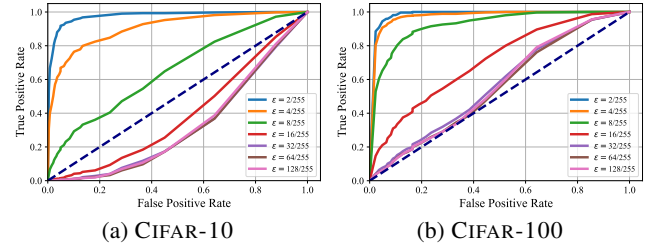


Figure 3: ROC Curve of BEYOND against adaptive attacks with different perturbation budgets.

Defense	$L_{\infty}=0.01$		$L_{\infty}=8/255$	
	RA@FPR5%	RA@FPR50%	RA@FPR5%	RA@FPR50%
BEYOND	88.38%	98.81%	13.80%	48.20%
BEYOND +ATC	96.30%	99.30%	94.50%	97.80%
Trapdoor	0.00%	7.00%	0.00%	8.00%
DLA’20	62.60%	83.70%	0.00%	28.20%
SID’21	6.90%	23.40%	0.00%	1.60%
SPAM’19	1.20%	46.00%	0.00%	38.00%

Table 6: Robust Accuracy under Orthogonal-PGD Attack.

ROC Curve of Perturbation Budgets. Fig. 3 summarizes the ROC curve varying with different perturbation budgets on CIFAR-10 and CIFAR-100. Our analysis regarding Fig. 3 is as follows: 1) BEYOND can be bypassed when perturbations are large enough, due to large perturbations circumventing the transformation. This proves that BEYOND is not gradient masking (Athalye, Carlini, and Wagner 2018) and our adaptive attack design is effective. However, large perturbations are easier to perceive. 2) When the perturbation is small, the detection performance of BEYOND for adaptive attacks still maintains a high level, because small perturbations cannot guarantee both label consistency and representation similarity (as shown in Fig. 4). The above empirical conclusions are consistent with the intuitive analysis in Sec. 3.3.

Performance against Orthogonal-PGD Adaptive Attacks Orthogonal-Projected Gradient Descent (Orthogonal-PGD) is a recently proposed AE detection benchmark. Orthogonal-PGD has two attack strategies: orthogonal strategy and selection strategy. Tab. 6 shows BEYOND outperforms the four baselines by a considerable margin in orthogonal strategy, especially under small perturbations. For the worst case, BE-

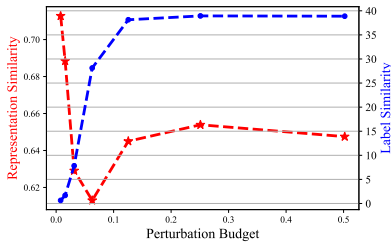


Figure 4: Trade-off between label consistency and representation similarity with perturbation budgets.

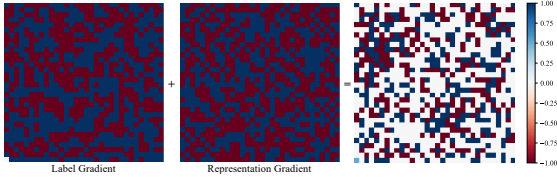


Figure 5: Gradient conflict between label consistency and representation similarity. The colored pixels represent the gradient direction, while the blank means gradient conflict.

YOND can still keep 13.8% ($L_\infty = 8/255$). Furthermore, incorporating ATC can significantly improve the detection performance of BEYOND against large perturbation to 94.5%. See Appendix for more selection strategy results.

Trade-off between label consistency and Representation Similarity The previous intuitive analysis and empirical results have proved that there is a trade-off between label consistency and representation similarity. Fig. 4 shows the variation of label consistency and representation similarity with perturbation size on CIFAR-100. We can observe that label consistency and representation similarity respond differently to the perturbation size and they can be optimized simultaneously only when the perturbation is large enough.

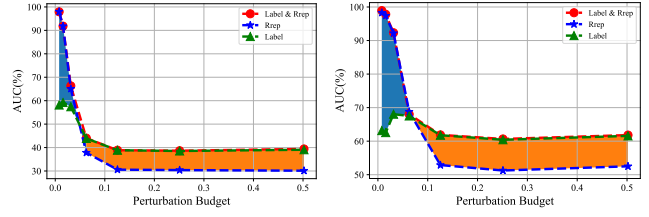
ϵ	2/255	4/255	8/255	16/255	32/255	64/255	128/255
s=0.002	55.92%	53.96%	52.32%	50.70%	50.73%	50.49%	50.36%
s=0.01	55.65%	52.91%	51.70%	48.53%	49.09%	49.09%	48.54%

Table 7: Gradient cancel ratio of perturbation budgets.

The conflict between label consistency and representation similarity stems from their different optimization direction. Fig. 5 visualizes the gradients produced by optimizing label consistency and representation similarity on the input. It's shown that attacks on label consistency or representation similarity produce gradients that modify the input in a certain direction, but optimizing for both leads to conflicting gradients. Tab. 7 counts the gradient conflict rates under a range of perturbation budgets with different step sizes. We can discover that large perturbations result in reduced gradient conflict rates, which validates our analysis again.

5.4 Ablation Study

We perform an ablation study on label consistency and representation similarity in CIFAR-10 and CIFAR-100, and an-



(a) CIFAR-10 (b) CIFAR-100
Figure 6: Ablation study on CIFAR-10 and CIFAR-100.

	Model	FLOPs(G)	Params(M)	Time(s)	Overall
ATC	R2021Fixing70	38.8	254.44	1.21	11945
	G2021Improving70	38.8	254.44	1.21	11945
	G2020Uncovering70	38.8	254.44	1.21	11945
	R2021Fixing106	60.57	396.23	1.24	29760
	BEYOND	<u>0.715</u>	<u>19.67</u>	<u>1.12</u>	<u>15.75</u>
Det.	LNG	0.28	7.95	9.22	<u>20.521</u>

Table 8: Comparison of time, computational and storage costs.

analyze their detection performance (AUC) under a wide perturbation budget in Fig. 6. When the perturbation is small, the detection performance based on label consistency (blue line) is better than representation similarity (green line). With increasing perturbation, representation similarity is difficult to maintain, leading to higher performance of representation similarity-based detectors, as same turning points as in Fig. 4. In summary, the label consistency and representation similarity have different sensitivities to perturbation, so their cooperation has the best detection performance (red line).

5.5 Implementation costs

BEYOND uses an additional SSL model for AE detection, which inevitably increases the computational and storage cost. And the inference time (speed) is also considered in practice. Tab. 8 presents the comparison for SOTA adversarial training defense and AE detection method, i.e. LNG. The detection models have a smaller model structure than those of ATCs, which can be reflected by the *Params* and *FLOPs* (Xie et al. 2020) being much lower than those of ATC. For BEYOND, the projection head is a three-layer FC, leading to higher parameters and *FLOPs* than LNG. However, BEYOND only compares the relationship between neighbors without calculating the distance with the reference set, resulting in a faster inference speed than that of LNG. We show the $FLOPs \times Params \times Time$ as the *Overall* metric in Tab. 8's last column for overall comparison. If cost is a real concern in some scenarios, we can further reduce the cost with some strategy, e.g., reducing the neighbor number, without compromising performance significantly, as shown in Fig. 2.

6 Conclusion

In this paper, we take the first step to detect AEs by identifying abnormal relations between AEs and their neighbors without prior knowledge of AEs. Samples have low label consistency, and representation similarity with their neighbors is detected as AE. Experiments with gray-box and white-box

attacks show that BEYOND outperforms the SOTA AE detectors in both detection ability and efficiency. Moreover, as a plug-and-play model, BEYOND can be well combined with ATC to further improve robustness.

References

- Abusnaina, A.; Wu, Y.; Arora, S.; Wang, Y.; Wang, F.; Yang, H.; and Mohaisen, D. 2021. Adversarial example detection using latent neighborhood graph. In *Proceedings of the IEEE/CVF International Conference on Computer Vision*, 7687–7696.
- Andriushchenko, M.; Croce, F.; Flammarion, N.; and Hein, M. 2020. Square Attack: A Query-Efficient Black-Box Adversarial Attack via Random Search. In *Computer Vision – ECCV 2020: 16th European Conference, Glasgow, UK, August 23–28, 2020, Proceedings, Part XXIII*, 484–501. Berlin, Heidelberg: Springer-Verlag. ISBN 978-3-030-58591-4.
- Athalye, A.; Carlini, N.; and Wagner, D. 2018. Obfuscated gradients give a false sense of security: Circumventing defenses to adversarial examples. In *International conference on machine learning*, 274–283. PMLR.
- Athalye, A.; Engstrom, L.; Ilyas, A.; and Kwok, K. 2018. Synthesizing robust adversarial examples. In *International conference on machine learning*, 284–293. PMLR.
- Bhatia, R.; and Davis, C. 1995. A Cauchy-Schwarz inequality for operators with applications. *Linear algebra and its applications*, 223: 119–129.
- Bryniarski, O.; Hingun, N.; Pachuca, P.; Wang, V.; and Carlini, N. 2021. Evading adversarial example detection defenses with orthogonal projected gradient descent. *arXiv preprint arXiv:2106.15023*.
- Carlini, N.; and Wagner, D. 2017. Towards evaluating the robustness of neural networks. In *2017 IEEE Symposium on Security and Privacy (SP)*, 39–57. Ieee.
- Chen, X.; and He, K. 2021. Exploring simple siamese representation learning. In *Proceedings of the IEEE/CVF Conference on Computer Vision and Pattern Recognition*, 15750–15758.
- Cococcioni, M.; Rossi, F.; Ruffaldi, E.; Saponara, S.; and de Dinechin, B. D. 2020. Novel arithmetics in deep neural networks signal processing for autonomous driving: Challenges and opportunities. *IEEE Signal Processing Magazine*, 38(1): 97–110.
- Croce, F.; Andriushchenko, M.; Sehwag, V.; Debenedetti, E.; Flammarion, N.; Chiang, M.; Mittal, P.; and Hein, M. 2020. Robustbench: a standardized adversarial robustness benchmark. *arXiv preprint arXiv:2010.09670*.
- Croce, F.; Goyal, S.; Brunner, T.; Shelhamer, E.; Hein, M.; and Cemgil, T. 2022. Evaluating the Adversarial Robustness of Adaptive Test-time Defenses. *arXiv preprint arXiv:2202.13711*.
- Croce, F.; and Hein, M. 2020. Reliable evaluation of adversarial robustness with an ensemble of diverse parameter-free attacks. In *International conference on machine learning*, 2206–2216. PMLR.
- da Costa, V. G. T.; Fini, E.; Nabi, M.; Sebe, N.; and Ricci, E. 2022. solo-learn: A Library of Self-supervised Methods for Visual Representation Learning. *J. Mach. Learn. Res.*, 23: 56–1.
- Demontis, A.; Melis, M.; Pintor, M.; Jagielski, M.; Biggio, B.; Oprea, A.; Nita-Rotaru, C.; and Roli, F. 2019. Why do adversarial attacks transfer? explaining transferability of evasion and poisoning attacks. In *28th USENIX security symposium (USENIX security 19)*, 321–338.
- Dubey, A.; van der Maaten, L.; Yalniz, I. Z.; Li, Y.; and Mahajan, D. 2019. Defense Against Adversarial Images using Web-Scale Nearest-Neighbor Search. *computer vision and pattern recognition*.
- Elfwing, S.; Uchibe, E.; and Doya, K. 2018. Sigmoid-weighted linear units for neural network function approximation in reinforcement learning. *Neural Networks*, 107: 3–11.
- Goyal, S.; Qin, C.; Uesato, J.; Mann, T.; and Kohli, P. 2020. Uncovering the limits of adversarial training against norm-bounded adversarial examples. *arXiv preprint arXiv:2010.03593*.
- Goyal, S.; Rebuffi, S.-A.; Wiles, O.; Stimberg, F.; Calian, D. A.; and Mann, T. A. 2021. Improving robustness using generated data. *Advances in Neural Information Processing Systems*, 34: 4218–4233.
- He, K.; Zhang, X.; Ren, S.; and Sun, J. 2016. Deep residual learning for image recognition. In *Proceedings of the IEEE conference on computer vision and pattern recognition*, 770–778.
- Hendrycks, D.; Mazeika, M.; Kadavath, S.; and Song, D. 2019a. Using self-supervised learning can improve model robustness and uncertainty. *Advances in neural information processing systems*, 32.
- Hendrycks, D.; Mazeika, M.; Kadavath, S.; and Song, D. 2019b. Using self-supervised learning can improve model robustness and uncertainty. *Advances in neural information processing systems*, 32.
- Ho, C.-H.; and Nvasconcelos, N. 2020. Contrastive learning with adversarial examples. *Advances in Neural Information Processing Systems*, 33: 17081–17093.
- Hu, S.; Yu, T.; Guo, C.; Chao, W.-L.; and Weinberger, K. Q. 2019. A New Defense Against Adversarial Images: Turning a Weakness into a Strength. *neural information processing systems*.
- Jaiswal, A.; Ramesh Babu, A.; Zaki Zadeh, M.; Banerjee, D.; and Makedon, F. 2020. A Survey on Contrastive Self-Supervised Learning.
- Jiang, Z.; Chen, T.; Chen, T.; and Wang, Z. 2020. Robust pre-training by adversarial contrastive learning. *Advances in Neural Information Processing Systems*, 33: 16199–16210.
- Kaissis, G.; Makowski, M.; Rückert, D.; and Braren, R. 2022. Secure, privacy-preserving and federated machine learning in medical imaging.
- Kim, M.; Tack, J.; and Hwang, S. J. 2020. Adversarial self-supervised contrastive learning. *Advances in Neural Information Processing Systems*, 33: 2983–2994.

- Krizhevsky, A.; Hinton, G.; et al. 2009. Learning multiple layers of features from tiny images.
- Krizhevsky, A.; Sutskever, I.; and Hinton, G. E. 2012. Imagenet classification with deep convolutional neural networks. *Advances in neural information processing systems*, 25.
- Liu, J.; Zhang, W.; Zhang, Y.; Hou, D.; Liu, Y.; Zha, H.; and Yu, N. 2019. Detection based defense against adversarial examples from the steganalysis point of view. In *Proceedings of the IEEE/CVF Conference on Computer Vision and Pattern Recognition*, 4825–4834.
- Liu, X.; Zhang, F.; Hou, Z.; Mian, L.; Wang, Z.; Zhang, J.; and Tang, J. 2021. Self-supervised learning: Generative or contrastive. *IEEE Transactions on Knowledge and Data Engineering*.
- Ma, X.; Li, B.; Wang, Y.; Erfani, S. M.; Wijewickrema, S.; Schoenebeck, G.; Song, D.; Houle, M. E.; and Bailey, J. 2018. Characterizing adversarial subspaces using local intrinsic dimensionality. *arXiv preprint arXiv:1801.02613*.
- Madry, A.; Makelov, A.; Schmidt, L.; Tsipras, D.; and Vladu, A. 2017. Towards deep learning models resistant to adversarial attacks. *arXiv preprint arXiv:1706.06083*.
- Mao, C.; Chiquier, M.; Wang, H.; Yang, J.; and Vondrick, C. 2021. Adversarial attacks are reversible with natural supervision. In *Proceedings of the IEEE/CVF International Conference on Computer Vision*, 661–671.
- Ma, C.; Gupta, A.; Nitin, V.; Ray, B.; Song, S.; Yang, J.; and Vondrick, C. 2020. Multitask learning strengthens adversarial robustness. In *European Conference on Computer Vision*, 158–174. Springer.
- Meng, D.; and Chen, H. 2017. Magnet: a two-pronged defense against adversarial examples. In *Proceedings of the 2017 ACM SIGSAC conference on computer and communications security*, 135–147.
- Mikołajczyk, A.; and Grochowski, M. 2018. Data augmentation for improving deep learning in image classification problem. In *2018 international interdisciplinary PhD workshop (IIPhDW)*, 117–122. IEEE.
- Papernot, N.; and McDaniel, P. 2018. Deep k-nearest neighbors: Towards confident, interpretable and robust deep learning. *arXiv preprint arXiv:1803.04765*.
- Papernot, N.; McDaniel, P.; and Goodfellow, I. 2016. Transferability in machine learning: from phenomena to black-box attacks using adversarial samples. *arXiv preprint arXiv:1605.07277*.
- Raff, E.; Sylvester, J.; Forsyth, S.; and McLean, M. 2019. Barage of random transforms for adversarially robust defense. In *Proceedings of the IEEE/CVF Conference on Computer Vision and Pattern Recognition*, 6528–6537.
- Rebuffi, S.-A.; Goyal, S.; Calian, D. A.; Stimberg, F.; Wiles, O.; and Mann, T. 2021. Fixing data augmentation to improve adversarial robustness. *arXiv preprint arXiv:2103.01946*.
- Shan, S.; Wenger, E.; Wang, B.; Li, B.; Zheng, H.; and Zhao, B. Y. 2020. Gotta Catch’Em All: Using Honey pots to Catch Adversarial Attacks on Neural Networks. *computer and communications security*.
- Shi, C.; Holtz, C.; and Mishne, G. 2021. Online adversarial purification based on self-supervision. *arXiv preprint arXiv:2101.09387*.
- Sitawarin, C.; Golan-Strieb, Z. J.; and Wagner, D. 2022. Demystifying the Adversarial Robustness of Random Transformation Defenses. In *International Conference on Machine Learning*, 20232–20252. PMLR.
- Sperl, P.; Kao, C.-Y.; Chen, P.; Lei, X.; and Böttinger, K. 2020. DLA: dense-layer-analysis for adversarial example detection. In *2020 IEEE European Symposium on Security and Privacy (EuroS&P)*, 198–215. IEEE.
- Svoboda, J.; Masci, J.; Monti, F.; Bronstein, M. M.; and Guibas, L. 2018. Peernets: Exploiting peer wisdom against adversarial attacks. *arXiv preprint arXiv:1806.00088*.
- Szegedy, C.; Zaremba, W.; Sutskever, I.; Bruna, J.; Erhan, D.; Goodfellow, I.; and Fergus, R. 2013. Intriguing properties of neural networks. *arXiv preprint arXiv:1312.6199*.
- Tian, J.; Zhou, J.; Li, Y.; and Duan, J. 2021. Detecting adversarial examples from sensitivity inconsistency of spatial-transform domain. In *Proceedings of the AAAI Conference on Artificial Intelligence*, volume 35, 9877–9885.
- Tramer, F. 2022. Detecting adversarial examples is (nearly) as hard as classifying them. In *International Conference on Machine Learning*, 21692–21702. PMLR.
- Tramèr, F.; Papernot, N.; Goodfellow, I.; Boneh, D.; and McDaniel, P. 2017. The space of transferable adversarial examples. *arXiv preprint arXiv:1704.03453*.
- Van der Maaten, L.; and Hinton, G. 2008. Visualizing data using t-SNE. *Journal of machine learning research*, 9(11).
- Wu, D.; Wang, Y.; Xia, S.-T.; Bailey, J.; and Ma, X. 2020. Skip connections matter: On the transferability of adversarial examples generated with resnets. *arXiv preprint arXiv:2002.05990*.
- Xie, C.; Tan, M.; Gong, B.; Wang, J.; Yuille, A. L.; and Le, Q. V. 2020. Adversarial examples improve image recognition. In *Proceedings of the IEEE/CVF Conference on Computer Vision and Pattern Recognition*, 819–828.
- Xu, W.; Evans, D.; and Qi, Y. 2017. Feature squeezing: Detecting adversarial examples in deep neural networks. *arXiv preprint arXiv:1704.01155*.
- Yang, Y.; Gao, R.; Li, Y.; Lai, Q.; and Xu, Q. 2022. What You See is Not What the Network Infers: Detecting Adversarial Examples Based on Semantic Contradiction. In *Network and Distributed System Security Symposium (NDSS)*.
- Zeng, Y.; Qiu, H.; Memmi, G.; and Qiu, M. 2020. A data augmentation-based defense method against adversarial attacks in neural networks. In *International Conference on Algorithms and Architectures for Parallel Processing*, 274–289. Springer.
- Zhang, H.; Yu, Y.; Jiao, J.; Xing, E.; El Ghaoui, L.; and Jordan, M. 2019. Theoretically principled trade-off between robustness and accuracy. In *International conference on machine learning*, 7472–7482. PMLR.